

Received 22 June; accepted 21 July 2000.

1. Mould, J. R. *et al.* The Hubble Space Telescope key project on the extragalactic distance scale. XXVIII. Combining the constraints on the Hubble constant. *Astrophys. J.* **529**, 786–794 (2000).
2. Weselink, A. J. Surface brightnesses in the U, B, V system with applications of M_V and dimensions of stars. *Mon. Not. R. Astron. Soc.* **144**, 297–311 (1969).
3. Krockenberger, M., Sasselov, D. D. & Noyes, R. W. Radii and distances of Cepheids. I. Method and measurement errors. *Astrophys. J.* **479**, 875–885 (1997).
4. Tanvir, N. R. in *Post-Hipparcos Cosmic Candles* 17–35 (Kluwer, Dordrecht, 1999).
5. Mourard, D. *et al.* The mean angular diameter of δ Cephei measured by optical long-baseline interferometry. *Astron. Astrophys.* **317**, 789–792 (1997).
6. Kervella, P. *et al.* in *Working on the Fringe: Optical and IR Interferometry from Ground and Space 22–27* (ASP Conf. Ser. 194, Astronomical Society of the Pacific, San Francisco, 1999).
7. Nordgren, T. *et al.* Astrophysical quantities of Cepheid variables measured with the NPOI. (in the press).
8. Szabados, L. Northern Cepheids: Period update and duplicity effects. *Commun. Konkoly Observatory, Hungary* **96**, 123–244 (1991).
9. Laney, C. D. & Stobie, R. S. The radii of galactic Cepheids. *Mon. Not. R. Astron. Soc.* **274**, 337–360 (1995).
10. Perryman, M. A. C. *et al.* The HIPPARCOS Catalogue. *Astron. Astrophys.* **323**, L49–L52 (1997).
11. Colavita, M. M. *et al.* The Palomar Testbed Interferometer. *Astrophys. J.* **510**, 505–521 (1999).
12. Colavita, M. M. Fringe visibility estimators for the Palomar Testbed Interferometer. *Publ. Astron. Soc. Pacif.* **111**, 111–117 (1999).
13. Boden, A. F. *et al.* An interferometric search for bright companions to 51 Pegasi. *Astrophys. J.* **504**, L39–L42 (1998).
14. Bersier, D., Burki, G., Mayor, M. & Duquennoy, A. Fundamental parameters of Cepheids. II. Radial velocity data. *Astron. Astrophys.* **108**, 25–39 (1994).
15. Hindsley, R. & Bell, R. A. An investigation of photoelectric radial-velocity spectrometers as used in the analysis of Cepheid variables. *Publ. Astron. Soc. Pacif.* **98**, 881–888 (1986).
16. Ridgway, S. T. *et al.* Angular diameters by the lunar occultation technique. IV—Alpha Leo and the Cepheid Zeta Gem. *Astron. J.* **87**, 680–684 (1982).
17. Gieren, W. P., Barnes, T. G. & Moffett, T. J. The period-radius relation for classical Cepheids from the visual surface brightness technique. *Astrophys. J.* **342**, 467–475 (1989).
18. Gieren, W. P., Barnes, T. G. & Moffett, T. J. The Cepheid period-luminosity relation from independent distances of 100 galactic variables. *Astrophys. J.* **418**, 135–146 (1993).
19. McAlister, H. A. *et al.* Progress on the CHARA array. *Proc. SPIE* **3350**, 947–950 (1998).
20. Cohen, M. *et al.* Spectral irradiance calibration in the infrared. X. A self-consistent radiometric all-sky network of absolutely calibrated stellar spectra. *Astron. J.* **117**, 1864–1889 (1999).
21. Welch, D. L. Near-infrared variant of the Barnes-Evans method for finding Cepheid distances calibrated with high-precision angular diameters. *Astron. J.* **108**, 1421–1426 (1999).
22. Claret, A., Diaz-Cordoves, J. & Gimenez, A. Linear and non-linear limb-darkening coefficients for the photometric bands R I J H K. *Astron. Astrophys.* **114**, 247–252 (1995).

Acknowledgements

We thank R. Akeson, T. Armstrong, A. Bouchez, M. Colavita, T. Nordgren, M. Nunez and D. Sasselov for valuable comments. Part of the work described in this paper was performed at the Jet Propulsion Laboratory under contract with the National Aeronautics and Space Administration. This research has made use of the Simbad database, operated at Centre de Données astronomiques de Strasbourg, Strasbourg, France. B.F.L. gratefully acknowledges the support of NASA through the Michelson fellowship programme. B.F.L. acknowledges the support of NASA and the NSF.

Correspondence and requests for materials should be addressed to B.F.L. (e-mail: bfl@astro.caltech.edu).

Simulating dynamical features of escape panic

Dirk Helbing*†, Illés Farkas‡ & Tamás Vicsek*‡

* Collegium Budapest—Institute for Advanced Study, Szentháromság u. 2, H-1014 Budapest, Hungary

† Institute for Economics and Traffic, Dresden University of Technology, D-01062 Dresden, Germany

‡ Department of Biological Physics, Eötvös University, Pázmány Péter Sétány 1A, H-1117 Budapest, Hungary

One of the most disastrous forms of collective human behaviour is the kind of crowd stampede induced by panic, often leading to fatalities as people are crushed or trampled. Sometimes this behaviour is triggered in life-threatening situations such as fires in crowded buildings^{1,2}; at other times, stampedes can arise during the rush for seats^{3,4} or seemingly without cause. Although engi-

neers are finding ways to alleviate the scale of such disasters, their frequency seems to be increasing with the number and size of mass events^{2,5}. But systematic studies of panic behaviour^{6–9} and quantitative theories capable of predicting such crowd dynamics^{5,10–12} are rare. Here we use a model of pedestrian behaviour to investigate the mechanisms of (and preconditions for) panic and jamming by uncoordinated motion in crowds. Our simulations suggest practical ways to prevent dangerous crowd pressures. Moreover, we find an optimal strategy for escape from a smoke-filled room, involving a mixture of individualistic behaviour and collective ‘herding’ instinct.

Up to now, panic as a particular form of collective behaviour occurring in situations of scarce or dwindling resources^{1,6} has been mainly studied from the perspective of social psychology^{7–9}. Panicking individuals tend to show maladaptive and relentless mass behaviour like jamming and life-threatening overcrowding^{1–4,8}, which has often been attributed to social contagion^{1,4,8} (see ref. 9 for an overview of theories). The observed jamming is a result of uncoordinated motion (‘incoordination’) and depends on the reward structure⁶.

We have studied related socio-psychological literature^{6–9}, reports in the media and available video materials (see <http://angel.elte.hu/~panic/>), empirical investigations^{1–3}, and engineering handbooks^{13,14}. The characteristic features of escape panics can be summarized as follows: (1) People move or try to move considerably faster than normal¹³. (2) Individuals start pushing, and interactions among people become physical in nature. (3) Moving and, in particular, passing of a bottleneck becomes uncoordinated⁶. (4) At exits, arching and clogging are observed¹³. (5) Jams build up⁷. (6) The physical interactions in the jammed crowd add up and cause dangerous pressures up to 4,450 N m⁻¹ (refs 2, 5) which can bend steel barriers or push down brick walls. (7) Escape is further slowed by fallen or injured people acting as ‘obstacles’. (8) People show a tendency towards mass behaviour, that is, to do what other people do^{1,8}. (9) Alternative exits are often overlooked or not efficiently used in escape situations^{1,2}.

These observations have encouraged us to model the collective phenomenon of escape panic in the framework of self-driven many-particle systems. Our computer simulations of the crowd dynamics of pedestrians are based on a generalized force model¹⁵, which is particularly suited to describing the fatal build up of pressure observed during panics^{2–5}. We assume a mixture of socio-psychological¹⁶ and physical forces influencing the behaviour in a crowd: each of N pedestrians i of mass m_i likes to move with a certain desired speed v_i^0 in a certain direction e_i^0 , and therefore tends to correspondingly adapt his or her actual velocity v_i with a certain characteristic time τ_i . Simultaneously, he or she tries to keep a velocity-dependent distance from other pedestrians j and walls W . This can be modelled by ‘interaction forces’ f_{ij} and f_{iW} , respectively. In mathematical terms, the change of velocity in time t is then given by the acceleration equation

$$m_i \frac{dv_i}{dt} = m_i \frac{v_i^0(t)e_i^0(t) - v_i(t)}{\tau_i} + \sum_{j \neq i} f_{ij} + \sum_W f_{iW} \quad (1)$$

while the change of position $r_i(t)$ is given by the velocity $v_i(t) = dr_i/dt$. We describe the psychological tendency of two pedestrians i and j to stay away from each other by a repulsive interaction force $A_i \exp[(r_{ij} - d_{ij})/B_i]n_{ij}$, where A_i and B_i are constants. $d_{ij} = ||r_i - r_j||$ denotes the distance between the pedestrians’ centres of mass, and $n_{ij} = (n_{ij}^x, n_{ij}^y) = (r_i - r_j)/d_{ij}$ is the normalized vector pointing from pedestrian j to i . The pedestrians touch each other if their distance d_{ij} is smaller than the sum $r_{ij} = (r_i + r_j)$ of their radii r_i and r_j . In this case, we assume two additional forces inspired by granular interactions^{17,18}, which are essential for understanding the particular effects in panicking crowds: a ‘body force’ $k(r_{ij} - d_{ij})n_{ij}$ counteracting body compression and a ‘sliding friction force’ $\kappa(r_{ij} - d_{ij})\Delta v_{ij}^t t_{ij}$ impeding relative tangential motion, if pedes-

trian i comes close to j . Here $\mathbf{t}_{ij} = (-n_{ij}^2, n_{ij}^1)$ means the tangential direction and $\Delta v_{ij}^t = (\mathbf{v}_j - \mathbf{v}_i) \cdot \mathbf{t}_{ij}$ the tangential velocity difference, while k and κ represent large constants. In summary, we have

$$\mathbf{f}_{ij} = \{A_i \exp[(r_{ij} - d_{ij})/B_i] + \kappa g(r_{ij} - d_{ij})\} \mathbf{n}_{ij} + \kappa g(r_{ij} - d_{ij}) \Delta v_{ij}^t \mathbf{t}_{ij} \quad (2)$$

where the function $g(x)$ is zero if the pedestrians do not touch each other ($d_{ij} > r_{ij}$), and is otherwise equal to the argument x .

The interaction with the walls is treated analogously: that is, if d_{iW} means the distance to wall W , \mathbf{n}_{iW} denotes the direction perpendicular to it, and \mathbf{t}_{iW} the direction tangential to it, the corresponding interaction force with the wall is given by:

$$\mathbf{f}_{iW} = \{A_i \exp[(r_i - d_{iW})/B_i] + \kappa g(r_i - d_{iW})\} \mathbf{n}_{iW} - \kappa g(r_i - d_{iW}) (\mathbf{v}_i \cdot \mathbf{t}_{iW}) \mathbf{t}_{iW} \quad (3)$$

Probably owing to the fact that escape panics are unexpected and dangerous events, which excludes real-life experiments, we could not find suitable data on escape panics to test our model quantitatively. This scarcity of data calls for reliable models. We have, therefore, specified the parameters as follows: with a mass of $m = 80$ kg, we represent an average soccer fan. The desired velocity v_i^0 can reach more than 5 m s^{-1} (up to 10 m s^{-1})¹⁴, but the observed free velocities for leaving a room correspond to $v_i^0 \approx 0.6 \text{ m s}^{-1}$ under relaxed, $v_i^0 \approx 1 \text{ m s}^{-1}$ under normal, and $v_i^0 \approx 1.5 \text{ m s}^{-1}$ under nervous conditions¹³. A reasonable estimate for the acceleration time is $\tau_i = 0.5$ s. With $A_i = 2 \times 10^3$ N and $B_i = 0.08$ m we can

reproduce the distance kept at normal desired velocities¹⁴ and fit the measured flows through bottlenecks¹⁴: specifically, 0.73 persons per second for an effectively 1-m-wide door under conditions with $v_i^0 \approx 0.8 \text{ m s}^{-1}$. The parameters $k = 1.2 \times 10^5 \text{ kg s}^{-2}$ and $\kappa = 2.4 \times 10^5 \text{ kg m}^{-1} \text{ s}^{-1}$ determine the obstruction effects in cases of physical interactions. Although, in reality, most parameters are varying individually, we chose identical values for all pedestrians to minimize the number of parameters for reasons of calibration and robustness, and to exclude irregular outflows because of parameter variations. However, to avoid model artefacts (gridlocks by exactly balanced forces in symmetrical configurations), a small amount of irregularity of almost arbitrary kind is needed. This irregularity was introduced by uniformly distributed pedestrian diameters $2r_i$ in the interval [0.5 m, 0.7 m], approximating the distribution of shoulder widths of soccer fans.

Based on the above model assumptions, we will now simulate several important phenomena of escape panic, which are insensitive to reasonable parameter variations, but fortunately become less pronounced for wider exits.

(1) Transition to incoordination due to clogging. The simulated outflow from a room is well coordinated and regular, if the desired velocities $v_i^0 = v_0$ are normal. But for desired velocities above 1.5 m s^{-1} , that is, for people in a rush, we find an irregular succession of arch-like blockings of the exit and avalanche-like bunches of leaving pedestrians when the arches break (Fig. 1a, b). This phenomenon is compatible with the empirical observations mentioned above, and comparable to intermittent clogging found

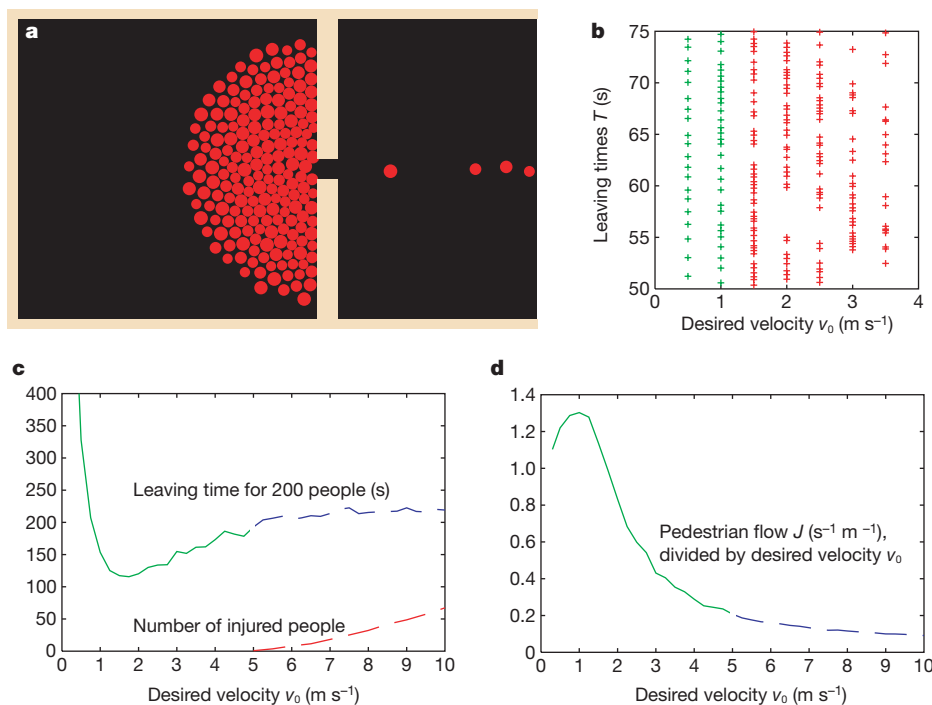


Figure 1 Simulation of pedestrians moving with identical desired velocity $v_i^0 = v_0$ towards the 1-m-wide exit of a room of size $15 \text{ m} \times 15 \text{ m}$. **a**, Snapshot of the simulation. Dynamic simulations are available at <http://angel.elte.hu/~panic/>. **b**, Leaving times of pedestrians for various desired velocities v_0 . Irregular outflow due to clogging is observed for high desired velocities ($v_0 \geq 1.5 \text{ m s}^{-1}$, red plus signs). **c**, Under conditions of normal walking, the time for 200 pedestrians to leave the room decreases with growing v_0 . Desired velocities higher than 1.5 m s^{-1} reduce the efficiency of leaving, which becomes particularly clear when the outflow J is divided by the desired velocity (**d**). This is due to pushing, which causes additional friction effects. Moreover, above a desired velocity of about $v_0 = 5 \text{ m s}^{-1}$ (corresponding to dashed lines in **c** and **d**) people are injured and become non-moving obstacles for others, if the sum of the magnitudes of the radial forces acting on them divided by their circumference exceeds a pressure of $1,600 \text{ N m}^{-1}$ (ref. 5).

Owing to the above 'faster-is-slower effect', panics can be triggered by pedestrian counterflows², which cause delays to the crowd intending to leave. This makes the stopped pedestrians impatient and pushy which may be described by increasing the desired velocity according to $v_i^0(t) = [1 - \rho_i(t)]v_i^0(0) + \rho_i(t)v_i^{\text{max}}$, where $v_i^0(0)$ is the initial, and v_i^{max} the maximum desired velocity. The time-dependent parameter $\rho_i(t) = 1 - \bar{v}_i(t)/v_i^0$, where $\bar{v}_i(t)$ denotes the average speed in the desired direction of motion, is a measure of impatience. Altogether, long waiting times increase the desired velocity, which can produce inefficient outflow. This further increases the waiting times, and so on, so that this tragic feedback can eventually trigger panics. It is therefore imperative to have sufficiently wide exits and to prevent counterflows when big crowds want to leave.

in granular flows through funnels or hoppers^{17,18}. (We note, however, that such clogging has been attributed to static friction between particles without remote interactions, and that the transition to clogging has been observed for small enough openings rather than for a variation of the driving force.

(2) ‘Faster-is-slower effect’ due to impatience. Since clogging is connected with delays, trying to move faster (that is, increasing v_i^0) can cause a smaller average speed of leaving, if the friction parameter κ is large enough (Fig. 1c, d). This effect is particularly tragic in the presence of fires, where fleeing people can reduce their own chances of survival. The related fatalities can be estimated by the number of pedestrians reached by the fire front (see <http://angel.elte.hu/~panic/>).

Because our friction term has, on average, no deceleration effect in the crowd, if the walls are sufficiently remote, the arching underlying the clogging effect requires a combination of two effects: first, slowing down due to a bottleneck such as a door, and second, strong inter-personal friction, which becomes dominant when pedestrians get too close to each other. Consequently, the danger of clogging can be minimized by avoiding bottlenecks in the construction of stadia and public buildings. We note, however, that jamming can also occur at widenings of escape routes. This surprising result is illustrated in Fig. 2. Improved outflows can be reached by columns placed asymmetrically in front of the exits, which also prevent the build up of fatal pressures (see <http://angel.elte.hu/~panic/>).

(3) Mass behaviour. We investigate a situation in which pedestrians are trying to leave a smoky room, but first have to find one of the invisible exits (see Fig. 3a). Each pedestrian i may either select an

individual direction \mathbf{e}_i or follow the average direction $\langle \mathbf{e}_j^0(t) \rangle_i$ of his neighbours j in a certain radius R_i (ref. 19), or try a mixture of both. We assume that both options are weighted with some parameter p_i :

$$\mathbf{e}_i^0(t) = \text{Norm}[(1 - p_i)\mathbf{e}_i + p_i\langle \mathbf{e}_j^0(t) \rangle_i] \quad (4)$$

where $\text{Norm}(\mathbf{z}) = \mathbf{z}/\|\mathbf{z}\|$ denotes normalization of a vector \mathbf{z} . As a consequence, we have individualistic behaviour if p_i is low, but herding behaviour if p_i is high. Therefore, p_i reflects the degree of panic of individual i .

Our model suggests that neither individualistic nor herding behaviour performs well (see Fig. 3b). Pure individualistic behaviour means that each pedestrian finds an exit only accidentally, while pure herding behaviour implies that the entire crowd will eventually move into the same and probably blocked direction, so that available exits are not efficiently used (Fig. 3d), in agreement with observations. According to Fig. 3b and c, we expect optimal chances of survival for a certain mixture of individualistic and herding behaviour, where individualism allows some people to detect the exits and herding guarantees that successful solutions are imitated by the others. If pedestrians follow the walls instead of ‘reflecting’ at them, we expect that herd following also causes jamming and inefficient use of doors (see Fig. 1), while individualists moving in opposite directions obstruct each other.

Our continuous pedestrian model is based on plausible interactions, and, owing to its simplicity, is robust with respect to parameter variations. Therefore, it is suitable for drawing conclusions about the possible mechanisms underlying the effects of escape panic (regarding an increase of the desired velocity, strong friction effects during physical interactions, and herding). After

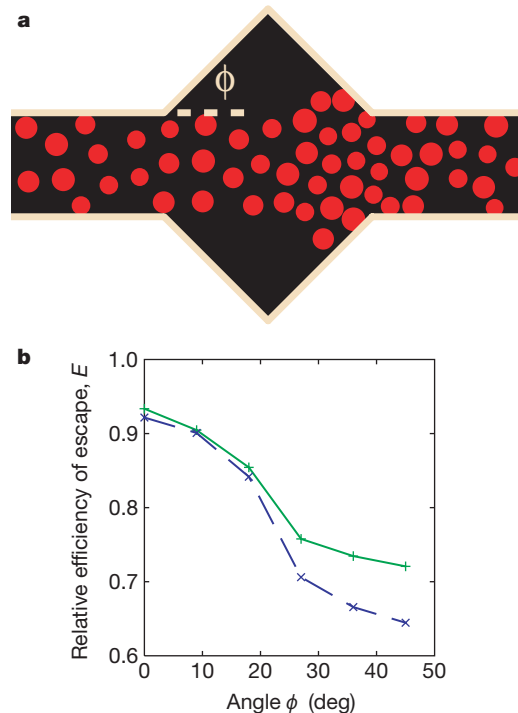


Figure 2 Simulation of an escape route with a wider area. **a**, Snapshot of the simulation with $v_i^0 = v_0 = 2 \text{ m s}^{-1}$. (Dynamic simulations are available at <http://angel.elte.hu/~panic/>) The corridor is 3 m wide and 15 m long, the length of the triangular pieces in the middle being $2 \times 3 \text{ m} = 6 \text{ m}$. Pedestrians enter the simulation area on the left-hand side with an inflow of $J = 5.5 \text{ s}^{-1} \text{ m}^{-1}$ and flee towards the right-hand side. **b**, Efficiency of leaving as a function of the angle ϕ characterizing the width of the central zone, that is, the difference from a linear corridor. The relative efficiency $E = \langle \mathbf{v} \cdot \mathbf{e}_i^0 \rangle / v_0$ measures the average velocity along the corridor compared to the desired velocity and lies between 0 and 1 (solid line). While it is almost one (that is, maximal) for a linear corridor ($\phi = 0$), the

efficiency drops by about 20% if the corridor contains a widening. This is understandable if we take into account that the widening leads to disturbances by pedestrians, who increase their separations in the wide area because of their repulsive interactions or try to overtake each other, and squeeze into the main stream again at the end of the widening. Hence the right half of the illustrated corridor acts like a bottleneck and leads to jamming. The drop of efficiency E is even more pronounced (1) in the area of the widening where pedestrian flow is most irregular (dashed line), (2) if the corridor is narrow, (3) if the pedestrians have different or high desired velocities, and (4) if the pedestrian density in the corridor is higher.

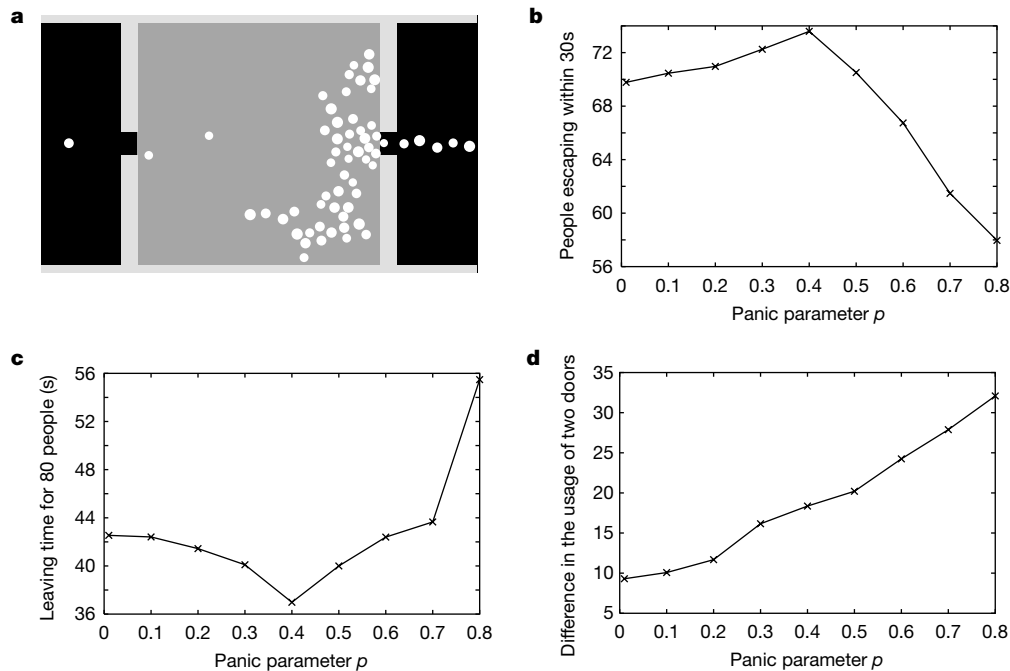


Figure 3 Simulation of $N = 90$ pedestrians trying to escape a smoky room of area $A = 15 \text{ m} \times 15 \text{ m}$ (grey) through two invisible doors of 1.5 m width. These doors have to be found with a mixture of individualistic and herding behaviour. Dynamic simulations are available at <http://angel.elte.hu/~panic/>. **a**, Snapshot of the simulation with $v_i^0 = v_0 = 5 \text{ m s}^{-1}$. Initially, each pedestrian selects his or her desired walking direction randomly. Afterwards, a pedestrian's walking direction is influenced by the average direction of the neighbours within a radius of, for example, $R_i = R = 5 \text{ m}$. The strength of this herding effect grows with increasing panic parameter $\rho_i = \rho$ and increasing value of $h = \pi R^2 \rho$, where $\rho = N/A$ denotes the pedestrian density. When reaching a boundary, the direction of a pedestrian is reflected. If one of the exits is closer than 2 m, the room is left. **b**, Number of people who manage to escape within 30 s as a function of the panic parameter ρ . **c**, Illustration of the time required by 80 individuals to leave the

smoky room. If the exits are relatively narrow and the panic parameter ρ is small or large, leaving takes a particularly long time, so that only some of the people escape before being poisoned by smoke. Our results suggest that the best escape strategy is a certain compromise between the following of others and an individualistic searching behaviour. This fits well with experimental data on the efficiency of group problem solving²⁰, according to which groups normally perform better than individuals, but masses are inefficient in finding new solutions to complex problems. **d**, Absolute difference $|N_1 - N_2|$ in the numbers N_1 and N_2 of persons leaving through the left exit or the right exit as a function of the panic parameter ρ . We find that pedestrians tend to jam up at one of the exits instead of equally using all available exits, if the panic parameter is large.

having calibrated the model parameters to available data on pedestrian flows, we have reproduced many observed phenomena. Our model could be used to test buildings for their suitability in emergency situations. Moreover, it accounts for the different dynamics in normal and panic situations by changing a single parameter $p_i = p$.

We are now calling for complementary data and additional video material on escape panics to test our model quantitatively, and compare it with alternative models. Such models could, for example, include direction- and velocity-dependent interpersonal interactions, specify the individual variation of parameters, study the effect of fluctuations, consider falling people, integrate acoustic information exchange, implement more complex strategies and interactions (also three-dimensional ones), or allow for switching of strategies. A superior theory would have to reproduce the empirical findings equally well with less parameters, reach a better quantitative agreement with data with the same number of parameters, or reproduce additional observations. \square

Received 2 June; accepted 31 August 2000.

- Keating, J. P. The myth of panic. *Fire J.* 57–61, 147 (May 1982).
- Elliott, D. & Smith, D. Football stadia disasters in the United Kingdom: learning from tragedy? *Ind. Environ. Crisis Q.* 7(3), 205–229 (1993).
- Jacobs, B. D. & 't Hart, P. in *Hazard Management and Emergency Planning* (eds Parker, D. J. & Handmer, J. W.) Ch. 10 (James & James Science, London, 1992).
- Johnson, N. R. Panic at "The Who Concert Stampede": an empirical assessment. *Soc. Problems* 34(4), 362–373 (1987).
- Smith, R. A. & Dickie, J. F. (eds) *Engineering for Crowd Safety* (Elsevier, Amsterdam, 1993).
- Mintz, A. Non-adaptive group behavior. *J. Abnormal Normal Social Psychol.* 46, 150–159 (1951).
- Kelley, H. H., Condry, J. C. Jr, Dahlke, A. E. & Hill, A. H. Collective behavior in a simulated panic

situation. *J. Exp. Social Psychol.* 1, 20–54 (1965).

- Quarantelli, E. The behavior of panic participants. *Sociol. Social Res.* 41, 187–194 (1957).
- Brown, R. *Social Psychology* (Free, New York, 1965).
- Drager, K. H. et al. in *Proc. 1992 Emergency Management and Engineering Conf.* (ed. Drager, K. H.) 101–108 (Society for Computer Simulation, Orlando, Florida, 1992).
- Ebihara, M., Ohtsuki, A. & Iwaki, H. A model for simulating human behavior during emergency evacuation based on classificatory reasoning and certainty value handling. *Microcomput. Civil Eng.* 7, 63–71 (1992).
- Still, G. K. New computer system can predict human behaviour response to building fires. *Fire* 84, 40–41 (1993).
- Predtetschenski, W. M. & Milinski, A. I. *Personenströme in Gebäuden—Berechnungsmethoden für die Projektierung* (Müller, Köln-Braunsfeld, 1971).
- Weidmann, U. *Transporttechnik der Fußgänger* (Institut für Verkehrsplanung, Transporttechnik, Straßen- und Eisenbahnbau (IVT), ETH Zürich, 1993).
- Helbing, D., Farkas, I. J. & Vicsek, T. Freezing by heating in a driven mesoscopic system. *Phys. Rev. Lett.* 84, 1240–1243 (2000).
- Helbing, D. & Molnár, P. Social force model for pedestrian dynamics. *Phys. Rev. E* 51, 4282–4286 (1995).
- Ristow, G. H. & Herrmann, H. J. Density patterns in two-dimensional hoppers. *Phys. Rev. E* 50, R5–R8 (1994).
- Wolf, D. E. & Grassberger, P. (eds) *Friction, Arching, Contact Dynamics* (World Scientific, Singapore, 1997).
- Vicsek, T., Czirók, A., Ben-Jacob, E., Cohen, I. & Schochet, O. Novel type of phase transition in a system of self-driven particles. *Phys. Rev. Lett.* 75, 1226–1229 (1995).
- Kelley, H. H. & Thibaut, J. W. in *The Handbook of Social Psychology* Vol. 4 (eds Lindzey, G. & Aronson, E.) (Addison-Wesley, Reading, Massachusetts, 1969).

Acknowledgements

D.H. thanks the German Research Foundation (DFG) for financial support by a Heisenberg scholarship. T.V. and I.F. are grateful for partial support by OTKA and FKFP.

Correspondence and requests for materials should be addressed to D.H. (e-mail: helbing@trafficforum.de).